STUDY OF ELECTRICAL CONDUCTIVITY IN CERAMIC FLOOR TILES. DEVELOPMENT OF AN ANITELELECTROSTATIC VITRIFIABLE GLAZE

J.V. Carceller(*), M.A. Jovaní(*), A. Nebot(*), A. Soler(*)
J. B. Carda(**), J.J. Gómez(**), G. García(***)
(*)COLOROBBIA ESPAÑA S.A.- Villafamés (Castellón)
(**)Dept. of Inorganic and Organic Chemistry. Universitat Jaume I
(***)Dept. of Experimental Science. Universitat Jaume I

ABSTRACT

Safety regulations in facilities where inflammable gases are handled or high voltage equipment is used require flooring with antielectrostatic characteristics according to Spanish regulations MIE BT 025. The present study showed that currently marketed glazed floor tile does not meet these requirements. This led to the development of vitrifiable stoneware floor tile glazes based on the incorporation of doped oxides of a semiconducting nature, which did conform to these requisites. This was done by testing two types of oxides: tin and titanium dioxide, both exhibiting rutile structure and it was shown that SnO_2 *presented a sufficiently low resistivity for these purposes, after doping with antimony oxide (*Sb_2O_3*).*

The developed conducting glazes were opaque and white, with resistivity values of around 10^6 *Ohm·cm, which lay within regulation range.*

Finally, the materials obtained were structurally and microstructurally characterised, confirming the entry of the antimony ion (III) in the cassiterite (SnO_2*) lattice.*

1. INTRODUCTION

In facilities where inflammable gases or explosive substances are handled special safety measures are required to prevent fire outbreaks. One such measure involves a minimum conductivity requirement in the flooring with a view to avoiding the accumulation of electrostatic charges. Electrostatic accumulation in these facilities can produce explosions by discharges that ignite inflammable gases, for example in operating theatres, explosive substances, or explosives magazines, stores with highly inflammable substances, etc. Moreover, recent studies, not directly focused on safety issues, have also found that the wellbeing of patients at hospitals and clinics improved noticeably when the facilities were fitted with antielectrostatic systems. They were also found to be recommendable in rooms containing computers or instruments sensitive to static electricity.

With a view to regulating the conductivity of the flooring used in facilities for which such security measures are requisite, the Ministry of Industry and Energy, in directive MIE BT 025 relative to facilities in premises accessible to the general public, requires that the flooring at such premises shall exhibit a maximum electrical resistance of 10^6 Ohm (1 MΩ). If it is certified that a higher value does not encourage the accumulation of hazardous electrostatic charges, the maximum admissible value becomes 100 MOhm. Regulations in other European countries also set similar requirements, in which the same electrical resistance values are specified for flooring in such facilities (DIN-51953 Germany, CNR-CEI n.64-4/73 Italy).

In view of these requirements, the present work had two objectives. One the one hand, characterisation of certain commercial flooring products to identify the situation regarding the current offer of such products. The characterisation was conducted from the point of view of the whole ceramic tile as a unit, and separately in terms of its individual constituents (ceramic body, engobe and glaze). On the other hand, on situating these different materials relative to the targeted conductivity, the second objective was to design materials, which on incorporation would provide the required characteristics for the function involved.

It is currently assumed that there is an arrangement on an atomic scale in glassy networks and even a "medium reach" below which glass and crystal topologies resemble each other quite closely, though they exhibit different geometries. Thus, some of the considerations concerning electrical conduction of crystalline solids are also applicable to glasses.

Electrical conductivity in ceramic materials made up of crystalline and glassy phases arises by two mechanisms: ionic conduction and electronic conduction.

Ionic conduction involves migration of charged ionic species across the material on applying an electrical field. Charge bearers are the more mobile ions. Ion migration can be divided into three types:

1. Vacancy mechanism: If there is a vacancy in the crystal lattice, it becomes possible for a neighbouring ion of the mobile type to move to this site. The difficulty of the movement lies in the size of the migrating ion and that of the surrounding ions, which attempt to hinder this. There is an energy barrier to be overcome in order to achieve this change of position, which will drop as the difference in ionic radii rises. This mechanism is related to Shottky defects (Fig. 1).

2. Interstitial mechanism: If an ion is small enough to occupy an interstitial position, such as for instance a tetragonal gap in an octahedral lattice, it can the move to other interstitial sites. This mechanism is related to Frenkel defects (Fig. 1).

3. Shifting mechanism to interstitial positions and creation of vacancies: This mechanism combines both the foregoing ones, in which an ion moves to an interstitial site from its original site in the lattice, thus producing a vacancy that can be occupied by another ion (Fig. 1).

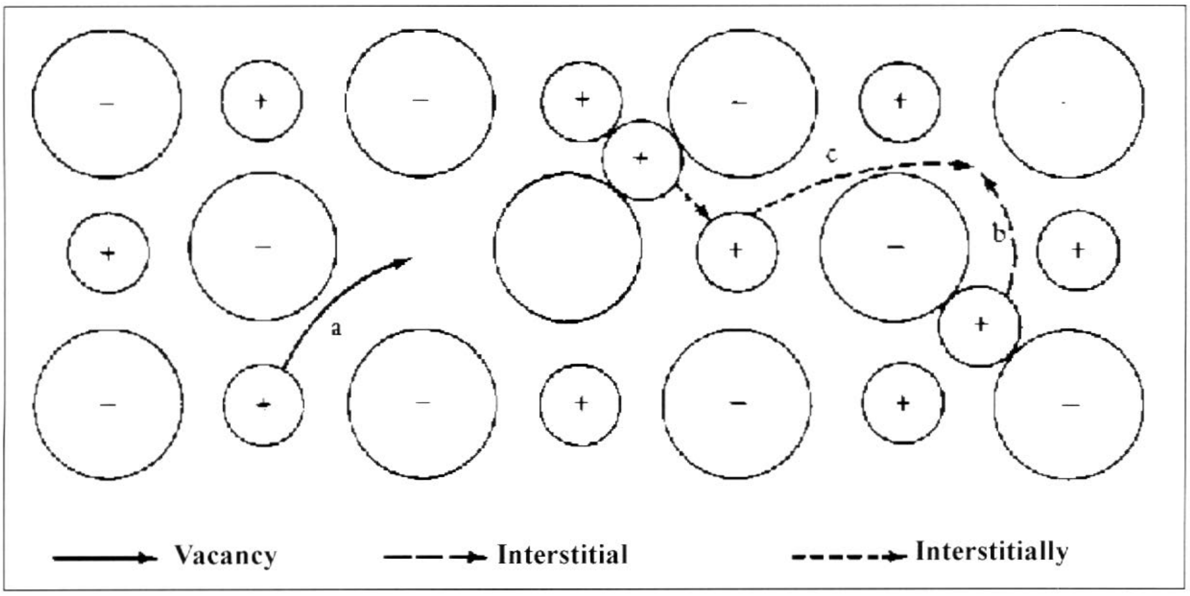

Fig. 1. *Schematic of the three ionic migration mechanisms a) Vacancy mechanism, b) Interstitial mechanism, c). Shifting mechanism to interstitial positions and creation of vacancies*

Lattice defects are natural in crystalline networks. However their number is limited and ruled by thermodynamic considerations (related to Boltzmann entropy), so that ionic conductivity is low. A way of fostering this is by introducing ions with a different charge from that of the matrix ions, so that charge compensation mechanisms will produce more crystalline defects.

Electronic conduction takes place by charge-bearing electrons. This type of conduction is explained by the energy band theory, according to which electrons take up a series of low energy levels, known as the valence band, and are able to promote to the immediately following higher energy levels, known as the conduction band. The ease with which the jump from one level to another is made indicates a material's behaviour with regard to electrical conduction, and this is related to the difference in energy exhibited by the two bands. In metals, which are excellent conducting materials, both bands lie close together. Insulators, as the opposite case, exhibit high energy differences, thus practically impeding these transitions, which is also the case of many ceramic materials. Many other materials such as the semiconductors lie in an intermediate situation, in which the magnitude of the electrical barrier, together with the presence of defects brought in by doping, provides an interesting conductivity. If these are doped with atoms containing one electron more than the matrix this favours the transition of more electrons into the conduction band, and n-type semiconductors are obtained. In this instance conduction takes place by negative bearers. If, however, atoms are brought in with an electron less, the concentration of positive gaps in the valence band rises. These are the p-type semiconductors with positive charge bearers. In the case at point, we are interested in ceramic semiconductors that can be obtained in traditional ceramic floor tile manufacture by current technology.

A material's electrical resistance to an electrical current is given by the following equation:

$$R = \rho \frac{L}{S} \qquad (1)$$

Where L is specimen length, S is conduction cross section area and ρ is electrical resistivity, which is defined as the electrical resistance of a cube of the material with a 1 cm edge. Thus, electrical resistance not only depends on the material involved, but also on its size. Although for the targeted function, the ceramic tile's electrical resistance was not to exceed a given maximum value, to carry out the study the material's behaviour needed to be assessed without considering its dimensions. The study was therefore conducted in terms of resistivity, as this fitted each material's nature better.

The inverse of resistivity is known as conductivity (τ):

$$\tau = \frac{1}{\rho} \qquad (2)$$

As glass conductivity varies with temperature according to an exponential Arrhenius-type equation up to temperatures close to the glass maturing range, rising as temperature climbs:

$$\tau = A \exp\left(\frac{-B}{T}\right) \qquad (3)$$

resistivity can be expressed as:

$$\rho = A' \exp\left(\frac{B}{T}\right) \qquad (4)$$

rewriting the equation and expressing it in a logarithmic form gives:

$$Log\ \rho = A'' + B''\left(\frac{1000}{T}\right) \qquad (5)$$

Where A and B are constants that depend on glass composition, while B corresponds to activation energy. These constants are not described theoretically here, as considerable literature is available elsewhere on the subject.

2. EXPERIMENTAL

As the ceramic materials used in tile manufacture generally exhibit clearly insulating behaviour, the phenomena of surface conduction associated with moisture retention at the surface are important. This surface conduction often exceeds that of the material itself. With a view to resolving the problem, the following measurement procedure was designed.

The ceramic specimens were heated in a thermostatted chamber in which the measurement was performed up to around 270-300 °C. After stabilising the temperature, the specimens were left to cool while an automated system took electrical resistance and temperature measurements. This yielded sufficient data to allow extrapolating, using Eqs. (1) and (5), and to thus obtain a value that approached the material's resistivity at room temperature, taken as 25 °C, in order to resolve the problems relating to surface moisture.

The procedure also allowed estimating the resistivity of highly insulating materials, which otherwise needed equipment capable of measuring resistance at quite high ranges (the equipment used presented a maximum range of $2 \cdot 10^{11}$ Ohms, 100,000 times greater than the targeted value).

As data extrapolation involves an inherent degree of uncertainty, two resistivity values were provided in each case, one obtained by extrapolation, and the other corresponding to the experimental reading at 110°C. As the specimen had already been heated and stabilised at a much higher temperature, no surface conduction relating to moisture was assumed to occur at 110 °C.

2.1. MATERIALS AND METHODS

Two types of specimens were analysed as far as their preliminary preparation was concerned. Commercial ceramic tiles were taken directly from the production line, once the manufacturing process had been completed, and prior to fitting with electrodes they were machined (cutting and polishing). The other specimens were obtained by the following process:

1. Selection of frit formulation.
2. Proportioning of frit raw materials.
3. Fritting at 1440 °C.
4. Proportioning of frit and additives.
5. Milling
6. Uniaxial powder pressing.
7. Firing the specimen according to a single-firing schedule in an industrial stoneware floor tile kiln.
8. Polishing and machining the specimen.
9. Fitting with platinum electrodes and resistivity measurement.

To characterise the materials the following instruments and techniques were used:

- KEITHLEY 617 programmable electrometer.
- Thermostatted chamber with range up to 1000 °C. Fitted with connections for two direct pressure electrodes and a thermocouple.

- SIEMENS, Model D5000, X-ray diffractometer running with a copper cathode and nickel filter, and secondary graphite monochromator, with automatic data processing. The measuring ranges ran from 10° to 70° (2θ).
- The resulting raw materials were analysed in a PHILIPS, Model PW2400, X-ray fluorescence spectrometer
- CARBOLITE electric kiln with a peak temperature of 1500 °C.
- Industrial floor tile kiln.
- PHILLIPS XL20, scanning electron microscope (SEM), with an energy-dispersive X-ray analysis system (EDAX).

Figure 2 depicts the preparation process used.

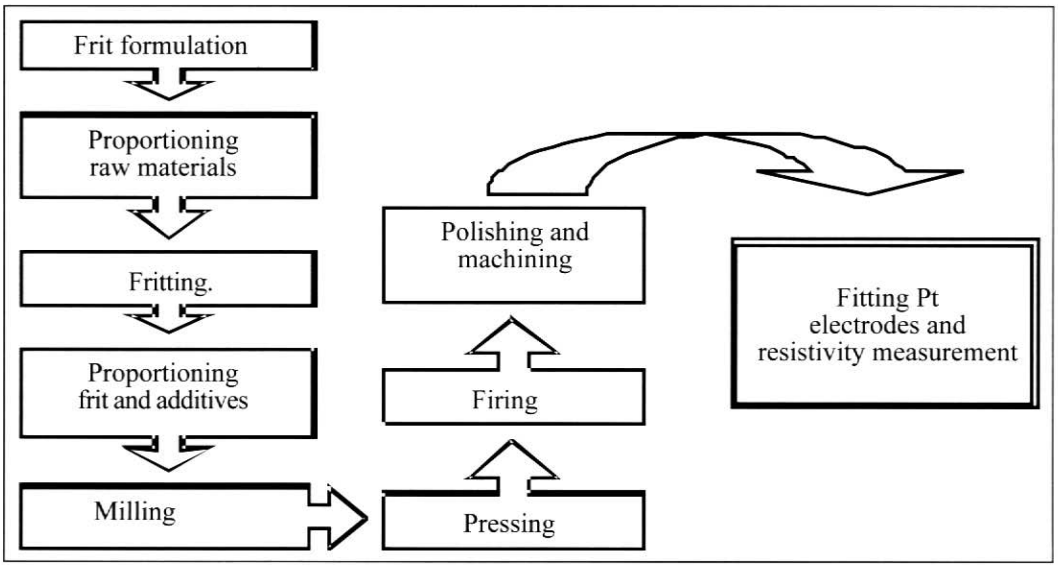

Figure 2. *Experimental scheme followed in specimen preparation up to measurement.*

Figure 3 illustrates the electrical measuring assembly.

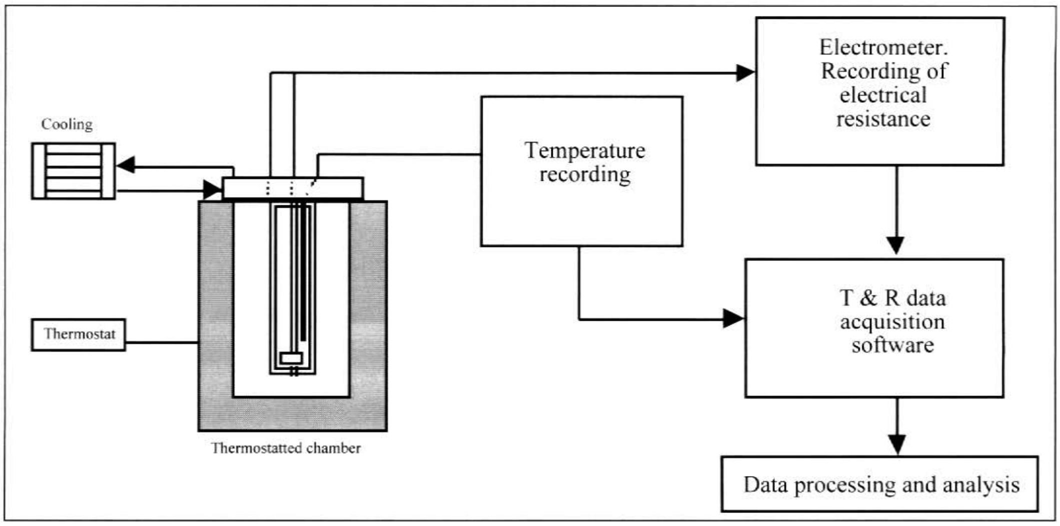

Figure 3. *Experimental electrical measuring assembly.*

3. RESULTS AND DISCUSSION.

3.1. CHARACTERISATION OF THE ELECTRICAL RESISTIVITY OF PORCELAIN TILE AND GLAZED STONEWARE, AS WELL AS THEIR CONSTITUENTS: BODY, ENGOBE AND GLAZE.

The first stage, as indicated, served to characterise commercial floor tiles. Industrially produced white and red stoneware tiles coated with two vitrifiable glazes of a different nature (a matt and a transparent glaze) were used for this purpose. Porcelain tile specimens without a stain addition were also analysed. The data are set out in Table I.

Table I	***Type of material***	***Glaze***	***Resistivity*** *of 110 ºC. (Ohms·cm)*	***Resistivity*** *extrapolated to 25 ºC. (Ohms·cm)*
White stoneware		Transparent	$8 \cdot 10^{9}$	$6 \cdot 10^{12}$
		Matt	$3 \cdot 10^{10}$	$4 \cdot 10^{12}$
Red stoneware		Transparent	$1.2 \cdot 10^{10}$	$1.1 \cdot 10^{13}$
		Matt	$1.1 \cdot 10^{11}$	$4 \cdot 10^{13}$
Porcelain tile		---	$3 \cdot 10^{9}$	$6 \cdot 10^{11}$

It can be observed that in the three cases, involving porcelain tile, glazed white and red stoneware tiles, conductivity values were found far above the regulation values.

The following step involved establishing the resistance of each ceramic tile component individually: body, engobe and glaze. In this step specimens were taken of the red and white stoneware bodies, a stoneware engobe and several vitrifiable glazes:

- Two vitrifiable opaque glazes: one with a zirconium and the other with a titanium opacifier.
- A transparent glaze with an alkaline-boric base.
- A barium matt glaze.

The results are detailed in Table II.

Table II	***Type of material***	***Resistivity*** *at 110° C. (Ohms·cm)*	***Resistivity*** *extrapolated to 25 ºC. (Ohms·cm)*
White stoneware body		$1 \cdot 10^{10}$ a $3 \cdot 10^{8}$ *	$2 \cdot 10^{12}$ a $1 \cdot 10^{10}$ *
Red stoneware body		$7 \cdot 10^{11}$ a $5 \cdot 10^{8}$ *	$3 \cdot 10^{13}$ a $3 \cdot 10^{10}$ *
Stoneware engobe		$4 \cdot 10^{8}$	$4 \cdot 10^{9}$
Zirconium opaque glaze		$3 \cdot 10^{10}$	$7 \cdot 10^{13}$
Titanium opaque glaze		$1.7 \cdot 10^{10}$	$4 \cdot 10^{10}$
· ***Transparent glaze***		$1.2 \cdot 10^{10}$	$1.4 \cdot 10^{10}$
Matt glaze		$4 \cdot 10^{8}$	$3 \cdot 10^{11}$

* The extreme values found are indicated.

The white and red stoneware bodies both exhibited high electrical resistivity. An appreciable variation was observed between their resistivities, which could be associated with the porosity and heterogeneity of these materials, aspects to be avoided in determining a material's conductivity, but which are inherent to ceramic materials. On the other hand, the effect of machining the specimens was noticeable: the polished fired specimens exhibited higher values than the specimens polished before firing.

Contrary to the white and red stoneware bodies, the porcelain tile specimens exhibited greater consistency in their resistivities as a result of lower porosity.

The studied engobe presented a slightly lower resistivity to the general trend shown by the studied vitrifiable glazes, and these in turn exhibited behaviour that varied markedly with the composition.

3.2. STUDY AND DEVELOPMENT OF THE GLAZE

After characterising the different materials, the following objective was to develop vitrifiable glaze that met the required conductivity conditions. The development of new bodies and engobes was left for a future study.

In view of the results and analysis of the compositions obtained for the studied glazes, the following inferences were drawn:

- The white zirconium glazes were found to lie in the most unfavourable position of the four studied types. They were thus discarded at the outset.
- There did not appear to be any appreciable differences between the other three glazes. However, the literature abundantly evinces the semiconducting properties of TiO_2 as well as of the other oxides of interest such as SnO_2, ZnO, Fe_2O_3, Cr_2O_3, etc.

It was decided to work with TiO_2 and SnO_2, which are used in ceramic glazes as opacifiers.

The opaque titanium glaze was used as the starting composition, whose base consisted of an opaque titanium frit, referenced FT, whose qualitative composition is detailed in Table III.

Table III	*SiO_2*	*Al_3O_2*	*B_3O_2*	*ZnO*	*CaO*	*MgO*	*Na_2O*	*K_2O*	*TiO_2*
FT wt%	55	5	5	10	10	3	1	5	6

This frit composition was subsequently modified by varying the titanium dioxide proportion, which was added as different proportions of anatase, both in the frit formulation as well as in the subsequent addition. Five compositions were prepared whose TiO_2 contents are detailed in Table IV.

Table IV	*FT1*	*FT2*	*FT3*	*FT4*	*FT5*
wt% (fusion)	6	9	0	6	3
wt% (addition)	0	0	6	3	3
Total TiO_2 wt%	6	9	6	9	6

The resistivities found for all these compositions, extrapolated to 25 °C, ranged from $2 \cdot 10^{10}$- $4 \cdot 10^{10}$. There was no significantly differentiated behaviour amongst the compositions. No noticeable improvements were obtained with regard to a decrease in resistivity in this range of TiO_2 percentages, whether in fusion or in the additions. Nor was there any appreciable enhancement of conductivity on raising the total percentage. Considering the data it was decided to replace this opacifier by tin dioxide.

Tin dioxide (SnO_2) is a well-known, widely used n-type semiconductor. It is used in the ceramic branch as an opacifier in producing white glazes. The most common crystalline form of this glaze is cassiterite, which belongs to the rutile crystallographic group, with a 6:3 coordination. It therefore crystallises in holohedral forms of the tetragonal system. It has a density of 6.8 at 7.1 g/cm^3 and a Mohs hardness of 6 to 7. In the natural state, it has a blackish colour, but the product used in ceramics is a semi-processed raw material and has a white colour. Figure 4 shows the cassiterite unit cell structure.

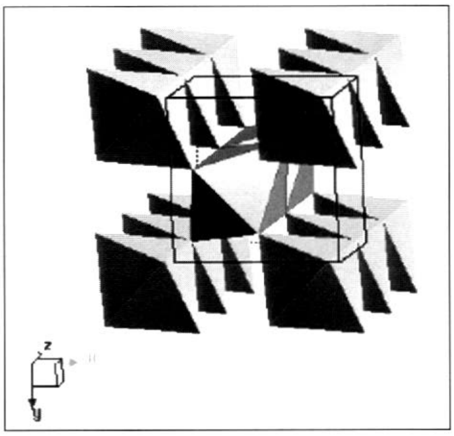

Fig 4. Cassiterite (SnO_2) structure. Cassiterite has a rutile type structure (TiO_2).

Compositions were prepared with tin dioxide from a commercial titanium frit (which appears in Table IV reference as FT1), eliminating the TiO_2 from its initial composition. Tin was subsequently added after fritting. To verify the effect on conductivity of the SnO_2 addition, the conductivity of the frit used (referenced F0) was also analysed. The compositions are set out in Table V.

Table V	***F0***	***FS1***	***FS2***
wt% SnO_2	0	6	35
wt% Frit (F0)	100	94	65

Composition FS1 (6% SnO_2) was formulated to compare the effect produced by tin dioxide compared to titanium dioxide; the weight equivalence corresponds to FT3 (6% TiO_2 addition). On the other hand, data reported in the literature involve high percentages of SnO_2, so that a formulation with 35% was used. The findings are set out on Table VI.

Table VI	***Resistivity*** ***at 110°C. (Ohms·cm)***	***Resistivity*** ***extrapolated to 25 °C. (Ohms·cm)***
F0	$1 \cdot 10^{10}$	$1.7 \cdot 10^{10}$
FS1	$1 \cdot 10^{8}$	$7 \cdot 10^{8}$
FS2	$5 \cdot 10^{9}$	$7 \cdot 10^{9}$

The data obtained in the literature indicate that conductivity should rise with increasing tin dioxide content. However, tin dioxide is quite a refractory material, so that adding high proportions to the frit substantially affects frit meltability. This seems to be the reason for the resistivity of formulation FS1 and la FS2 (6 and 35% SnO_2 respectively) not exhibiting the expected tendency.

A considerable improvement in conductivity can be observed on replacing TiO2 by SnO_2. The resulting conductivity obtained with the tin dioxide addition also improved compared to the starting frit value. Nevertheless, the resistivities were not sufficient, not even on employing considerable SnO_2 proportions. To enhance these values recourse was had to doping tin dioxide.

3.3. STUDY AND DEVELOPMENT OF A GLAZE BASED ON DOPING TIN DIOXIDE

Data can be found in the literature on SnO_2 doped with Sb(III), Cu(II), Zn, V(III and V), Bi(III) oxides, etc. At this stage it was attempted to improve the conductivity values of the vitrifiable glaze starting out from frit F0, to which doped tin dioxide was added. The entry of doping agents was provoked in SnO_2 to produce crystalline defects in the cassiterite lattice, which as mentioned in the introduction lead to greater conductivity.

Mixtures were prepared of tin oxide and the doping agent, which were heat-treated at 1350 °C for an hour. These were subsequently added to the reference composition (F0) in a weight ratio of 65% frit and 35% calcined blend of tin oxide and doping agent. Table VII details the compositions.

Table VII wt%	***FSb***	***FBi***	***FV***	***FLi***
% SnO_2	33	31.9	33.7	9
% Sb_2O_3	2	--	--	--
% Bi_2O_3	--	3.1	--	--
% V_2O_5	--	--	1.3	--
% Li_2O	--	--	--	1
% F0	65	64.3	65	90

The results are given in Table VIII:

Table VIII	***Resistivity at 110°C. (Ohms·cm)***	***Resistivity extrapolated to 25 °C. (Ohms·cm)***
FSb	$3{\cdot}10^{6}$	$1.4{\cdot}10^{7}$
FBi	$4{\cdot}10^{10}$	$9{\cdot}10^{10}$
FV	$5{\cdot}10^{10}$	$1.4{\cdot}10^{11}$
FLi	$3{\cdot}10^{10}$	$1.4{\cdot}10^{11}$

It can be observed that the specimens doped with bismuth (III), vanadium (V) and lithium oxide did not improve on the conductivity previously reached with composition FS2. However, the specimen doped with antimony (III) oxide did exhibit an appreciable improvement. The resulting product was a grey colour (a ceramic grey colour is currently available of tin-antimony).

A series of compositions was prepared in which the effect was monitored of incorporating fritted or subsequently added tin dioxide, as well as seeking an optimum SnO_2/Sb_2O_3 ratio For this purpose, the tin and antimony oxides were fritted together with the other oxides in the reference frit. These compositions are detailed in Table IX.

Table IX ***wt%***	***FS2***	***FS3***	***FS4***	***FS5***	***FS6***
% SnO_2	35 addition	35 fusion	34	33	32
% Sb_2O_3	0	0	1	2	3
% F0	65	65	65	65	65

The resistivities obtained are reported in Table X.

Table X	***Resistivity*** ***at 110°C. (Ohms·cm)***	***Resistivity*** ***extrapolated to 25 °C. (Ohms·cm)***
FS2	$5 \cdot 10^{9}$	$7 \cdot 10^{9}$
FS3	$5 \cdot 10^{10}$	$1.5 \cdot 10^{11}$
FS4	$3 \cdot 10^{8}$	$9 \cdot 10^{8}$
FS5	$3 \cdot 10^{8}$	$1 \cdot 10^{9}$
FS6	$5 \cdot 10^{10}$	$8 \cdot 10^{10}$

The resistivities found with these compositions did not meet regulation requirements. However, certain conclusions were to be drawn.

With regard to the evolution of conductivity with the SnO_2/Sb_2O_3 ratio, on raising the ratio, resistivity dropped to a minimum between ratios 34/1 and 33/2, after which it started increasing. The frits all exhibited a grey colour.

Considering the results of frits FS2 and FS3, it can be observed that the resulting conductivity was higher on adding SnO_2 directly instead of incorporating it in fritting. Figures 5 and 6 present SEM images of specimens FS2 and FS3 (35% SnO_2 as a direct addition and in the melt respectively), showing the difference in SnO_2 distribution. For the molten specimen the distribution was much more uniform as a result of fritting and this difference might be the cause of the difference in behaviour. Thus, on incorporating SnO_2 directly without fritting, a better result was obtained as regards conductivity, while also simplifying frit processing as this oxide is very refractory (fusion T of 1650 °C). Antimony (III) oxide was added in fritted form as it produced problems as a result of degassing.

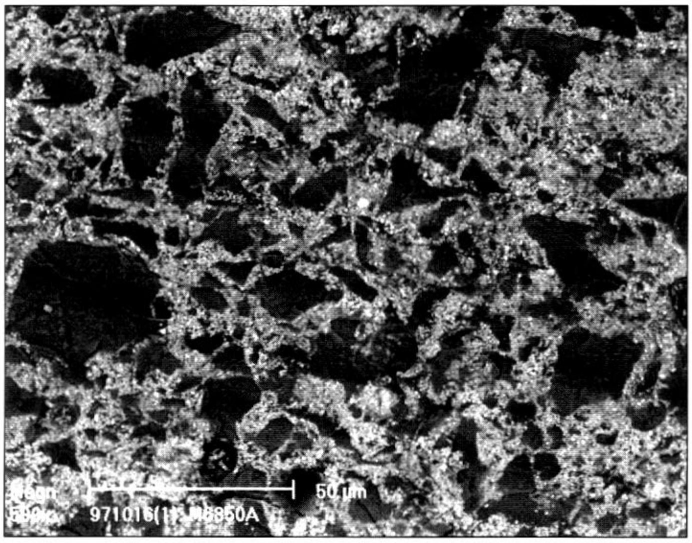

Figure 5. *SnO_2 by direct addition*

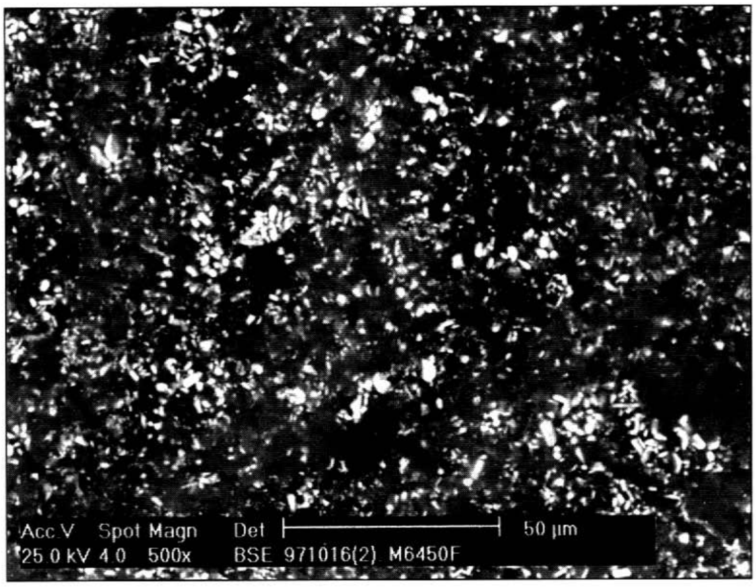

Figure 6. *SnO_2 in fusion.*

A series of specimens was therefore prepared in which tin was subsequently added and antimony was incorporated in the fitting process together with the other composition oxides; these frits were referenced FSb (their composition varied in terms of the Sb_2O_3 %). The composition proportions of SnO_2 and the frit, as well as the resistivities found, are reported in Tables XI and XII respectively.

Table XI ***wt%***	***FS7***	***FS8***	***FS9***
% SnO_2 addition	34	33	32
% Sb_2O_3 in frit FSb	1	2	3
% FSb	66	67	68

Table XII	***Resistivity*** ***at 110°C. (Ohms·cm)***	***Resistivity*** ***extrapolated to 25 °C. (Ohms·cm)***
FS7	$4 \cdot 10^4$	$6 \cdot 10^5$
FS8	$2 \cdot 10^5$	$5 \cdot 10^6$
FS9	$8 \cdot 10^4$	$1 \cdot 10^6$

It can be observed that for the three studied compositions, the resulting resistivity lay in a range that met regulation specifications for the facilities described in the introduction, with regard to the glaze.

A white product was obtained, fritting was facilitated and properties were held steady, while obtaining a product with sufficiently low resistivity for the targeted function.

The improvement in conductivity with regard to the values obtained for the compositions only containing tin dioxide was related to the entry of Sb^{+3} ions in the cassiterite lattice. This doping, as the ionic radii of Sn^{+4} (0.69 angstrom) and Sb^{+3}(0.80 angstrom) are different, produced a lattice distortion that can be appreciated in the shift in characteristic cassiterite lattice peaks in respect of the standard, (File 41-1445 JCPDS Cassiterite) in the XRD of Figure 7.

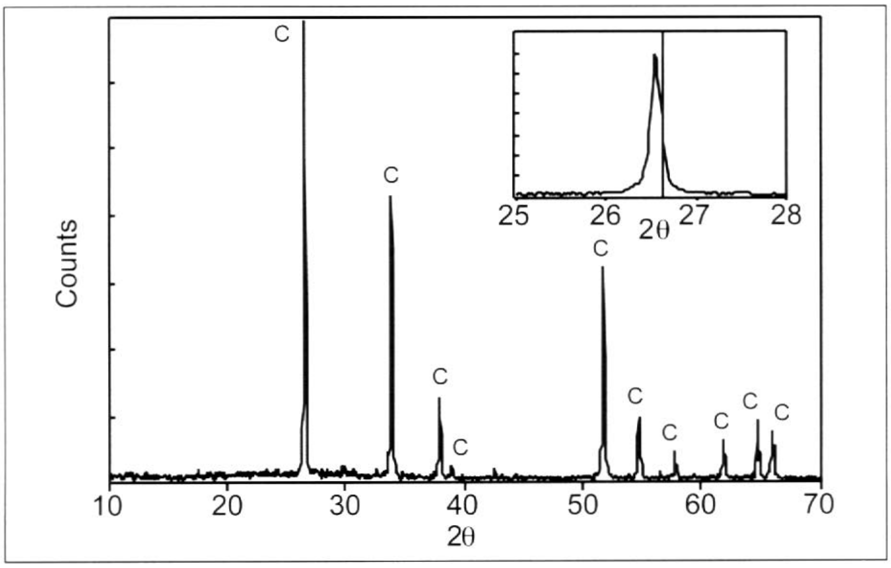

Fig 7. XRD of composition FS8 (33% SnO_2 addition, 2 % fritted Sb_2O_3), in which only the cassiterite crystalline phase was identified (41-1445), together with peak shift. C: Cassiterite.

As the cost of SnO_2 was a factor to be considered, the total proportion of SnO_2 was reduced in order to optimise it. Two compositions were prepared with SnO_2 doped with Sb_2O_2, taking the relative tin and antimony oxide composition of 33/2 (corresponding to composition FS8) and keeping it steady, as this was considered to approach the optimum ratio. The compositions and results are detailed in Tables XIII and XIV.

Table XIII **wt%**	**FS10**	**FS11**
% SnO_2 addition	10	25
% Sb_2O_3 in frit FSb	0.6	1.5
% FSb	89.4	73.5

Table XIV	**Resistivity at 110°C. (Ohms·cm)**	**Resistivity extrapolated to 25 °C. (Ohms·cm)**
FS10	$3 \cdot 10^7$	$1.6 \cdot 10^9$
FS11	$9 \cdot 10^4$	$1.4 \cdot 10^6$

The tendency exhibited by the results indicates that raising the overall SnO_2-Sb_2O_3 content improved glaze conductivity.

The composition with 25% tin dioxide and the antimony (III) oxide proportion corresponding to 33/2 exhibited a conductivity of the same order as that obtained for compositions FS7 to FS9. The reduction in the total SnO_2 percentage was therefore feasible.

Figure 8 shows the evolution of electrical resistivity with temperature for specimens FS7 to FS9. The figure reveals that the dependence of resistivity on temperature allows estimating the resistivity value at room temperature with a certain degree of confidence. Figure 9 plots the resistivity values versus the SnO_2 proportions in compositions FS2 (0% SnO_2), FS10 (10% SnO_2), FS11 (25% SnO_2) and FS8 (35% SnO_2).

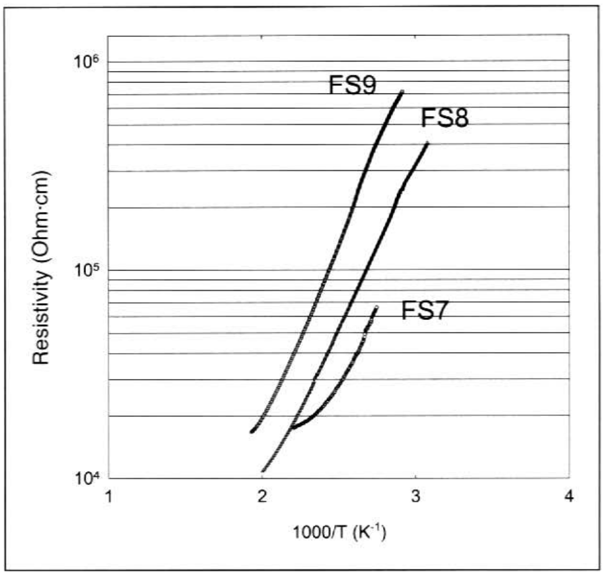

Fig. 8 *Resistivity &. 1000/T of the last two series.*

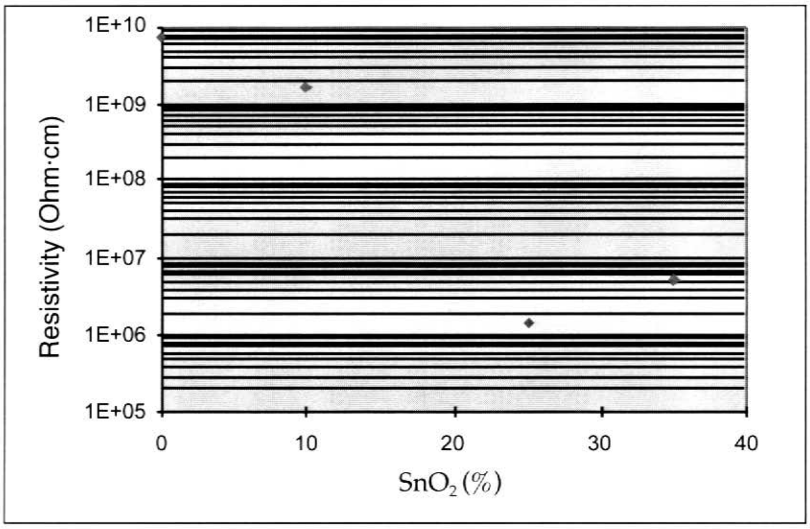

Fig. 9 *Resistivity vs. SnO_2 %.*

4. CONCLUSIONS

Three types of floor tiles were characterised, a white and a red stoneware tile, and porcelain tile. It was shown that current conventional products do not meet the conductivity requirement stipulated in the MIE BT 025 regulations.

A composition was obtained and a method developed for preparing a vitrifiable glaze that met antielectrostatic requirements, based on the system SnO_2-Sb_2O_3, which was classified as an opaque, white glaze.

In spite of not having obtained satisfactory results in doping tin dioxide with other oxides, this does not exclude other compositions from possibly doing better. There remains the possibility of using different proportions, doping TiO_2 or employing other semiconducting oxides.

5. REFERENCES

1. FERNÁNDEZ, J.M.: El vidrio. CSIC. *Fundación Centro Nacional del Vidrio. Real Fabrica de Cristales de la Granja*. Madrid, 1991.

2. HENC, L.L.; West J.L.: *Principles of electronic ceramics*. John Wiley & Sons. New York, 1990.

3. MAUSON, A.J.; HERBERT, J.M.: *Electroceramics materials, properties and applications*. Chapman & Hall. London, 1993.

4. HUHEEY J.E.; KEITER E.A.; KEITERR.L.: *Inorganic chemistry. Principles of structure and reactivity*. Harper Collins College Publishers, 1993.

5. RICHERSON D.W.: *Modern ceramic engineering. Properties, processing, and use in design*. Marcel Dekker, New York, 1992.

6. JURADO, J.R.: *Propiedades de materiales cerámicos avanzados: Propiedades eléctricas*. Cerámica Información 209 (1996), 13-23.

7. LOCH L.D.: *Semiconducting Nature Of Stannic Oxide*. J. Electrochem. Soc, 110 1081 (1963)

8. ZUCA, S.; MIHIU, S.; ZAHARESCU, M.: *Electrical properties of the ceramics in the Sn-Sb-Cu-O system*. Fourth Euro Ceramics Vol 5, 373-380.

9. ZAHARESCU, M.; MIHIU, S.; ZUCA, S.: *Contribution to the study of* SnO_2*-based ceramics. Part I. High-temperature interaction of tin (IV) oxide with antimony (III) oxide and copper (II) oxide.* J. Mat. Science, 26, 1666-1672, 1991.

10. ZUCA, S.; TERZI, M.;ZAHARESCU, M.; MATIASOYSKY, K.: *Contribution to the study of* SnO_2*-ceramics. Part II. Effect of various oxide additives on the sintering capacity and electrical conductivity of* SnO_2.

11. SAHAR, M. R., HASBULLAH, M. *Properties of the* SnO_2*-based ceramics*. Third Euro Ceramics Vol 2, 455-460.

12. PARIA, M.K.; MAITI, H.S.: *Electrical conductivity and defect structure of polycrystalline tin dioxide doped with antimony oxide*. J. Mater. Sci. 17 (1982) 3275.